Lattice dynamics of crystals with tetragonal $BaTiO_3$ structure

J. D. Freire
Departamento de Física, Universidade Federal de São Carlos, São Carlos, São Paulo, Brazil

R. S. Katiyar*
Department of Physics, University of Puerto Rico, Rio Piedras Campus, San Juan, Puerto Rico 00931
(Received 11 May 1987)

A lattice-dynamical formalism using the rigid-ion model due to Born and Huang is applied to the ferroelectric crystals $PbTiO_3$ and $BaTiO_3$, in the tetragonal phase. The model includes short-range interactions of axially symmetric type between various ions in the primitive cell and long-range Coulomb interactions. The stability conditions are worked out in the manner described by Katiyar and are used to determine several first-order derivative potential constants for the crystals. The number of potential constants was further reduced by considering the variation of radial force constants with the ion-ion distance, as given by the exponential formalism of Born and Mayer. Zone-center phonons and a few of the low-frequency zone-boundary phonons were used for the nonlinear least-squares fitting. In general, we obtained excellent agreement between the calculated and observed frequencies. The resulting parameters showed that the short-range interaction between the nearest titanium and oxygen is approximately 1 order of magnitude stronger than the interactions between the lead and oxygen or between the oxygens. The calculations showed that the lowest transverse-optic mode of E symmetry in $PbTiO_3$ has eigenvectors similar to those predicted by Last, whereas in $BaTiO_3$ the ionic movement in the lowest optic E mode can be approximated by the description of Slater. The phonon dispersion curves for various directions of the wave vector q were computed. These results are in good agreement with the inelastic neutron measurements by Shirane *et al.* A calculation of the oblique phonons near the zone center is presented and compared with the available experimental data. These calculations show that the long-range Coulomb forces dominate the anisotropic forces in these crystals. A theoretical approach for computing the elastic, dielectric, and piezoelectric properties is presented and the proposed model applied for calculating these constants. The results are compared with the experimental data where existed. Finally, a least-squares analysis of the observed phonons in $PbTiO_3$ near the tetragonal-cubic phase-transition temperature was carried out to understand the influence of anharmonic forces and the mechanism of the phase transition in this crystal. In general, the variation in the parameters obtained is very small. This shows that the small anharmonic forces may be sufficient to explain the variation of frequencies with temperature.

I. INTRODUCTION

Crystals of the perovskite family, such as $PbTiO_3$, $BaTiO_3$, $CaTiO_3$, etc., have been of constant interest in physics because some of these materials show ferroelectric behavior and undergo structural phase transitions.[1,2] $BaTiO_3$ may be considered one of the most studied crystal of this family. Above 120 °C it is cubic and belongs to space group $Fm3m$ (O_h^1). At temperatures below 120 °C it is ferroelectric and its structure is $P4mm$ (C_{4v}^1). If the temperature is lowered further the crystals of $BaTiO_3$ undergo new structural transitions at 5 °C and −90 °C, transforming to orthorhombic and trigonal symmetries, respectively. A number of researchers have studied the temperature-dependent vibration spectra of this material[3–9] utilizing Raman and infrared spectroscopic techniques. There are, however, conflicting reports with regard to the interpretation of their experimental observations in relation to the applicability of so-called "soft-mode theory" originally proposed by Cochran[10] and Anderson[11] independently in order to explain the anomalous dielectric behavior and the structural phase transition in ferroelectric materials.

Another important crystal of the perovskite family is $PbTiO_3$. Like $BaTiO_3$ this crystal is also ferroelectric at room temperature and it undergoes a tetragonal-cubic phase transition[12,13] at 493 °C, similar to that observed in $BaTiO_3$ at 120 °C. The Curie-Weiss temperature[14] of this crystal is 449 °C showing that the 493 °C transition is weakly first order. Dielectric-constant measurements of powder samples of $PbTiO_3$ showed small anomalies[15,16] for temperatures near −100 °C and −150 °C and these authors suggested a possible antiferroelectric transition at −100 °C in $PbTiO_3$. According to a recent x-ray study[17] $PbTiO_3$ undergoes a phase transition at −90 °C from cubic C_{4v} point-group symmetry to C_{2v}.

Experimental studies of phonons in $PbTiO_3$ were carried out[18–28] using Raman, infrared, or neutron scattering techniques. These studies showed that the lattice modes in $PbTiO_3$ are sharp and underdamped even in the vicinity of the transition temperature. Experimental studies of elastic and piezoelectric properties have been

made only in the polycrystalline samples[29–31] of $PbTiO_3$. Bhide *et al.*[32] have, however, measured the component ϵ_{33} of the dielectric tensor.

In the present work we make a theoretical study of phonons and the elastic and piezoelectric properties of crystals of $PbTiO_3$ and $BaTiO_3$ in the tetragonal phase. The temperature variation of the zone-center phonon frequencies and the oblique phonon dispersion curves are also computed. A rigid-ion model with long-range Coulomb forces and short-range axially symmetric forces with some approximations are used to describe the above properties.

II. CRYSTAL STRUCTURE AND NORMAL-MODE SYMMETRIES

The tetragonal form of $PbTiO_3$ has one formula unit in the primitive cell. Its space group is $P4mm$ (C_{4v}^1) and the ions occupy the following positions in the primitive cell:[33] Pb, (O,O,O); Ti, $(\frac{1}{2},\frac{1}{2},u)$; O(1), $(\frac{1}{2},\frac{1}{2},v)$; O(2), $(\frac{1}{2},O,w)$; and O(3), $(O,\frac{1}{2},w)$, where $u=0.541$, $v=0.112$, and $w=0.612$. The room-temperature lattice parameters[34] for the tetragonal cell are $a_0=3.904$ Å and $c_0=4.150$ Å.

Barium titanate is isomorphous to $PbTiO_3$ in the tetragonal phase[35] with the structural parameters $u=0.513$, $v=-0.0023$, and $w=0.487$. The lattice parameters for the room-temperature structure[36] are as follows: $a_0=3.992$ Å and $c_0=4.036$ Å. For lattice-dynamical calculations it is convenient to introduce an identification index for each ion in the primitive cell. We have, therefore, assigned the following indices for the ions:

ions	Pb	Ti	O(1)	O(2)	O(3)
indices	1	2	3	4	5

Figure 1 shows various critical points in the Brillouin zone. Following Montgomery,[37] we have classified the normal modes of vibrations for various high-symmetry critical points in the Brillouin zone and they are listed in Table I. The ions involved in a particular normal mode of vibration are in parentheses and the subscripts denote the direction of mode vibration. The basis vectors can be obtained using the projection-operator technique[37] and they are listed in Table II. The normal modes of vibrations are the linear combinations of these basis vectors with the linear constants involving the force-constant parameters.

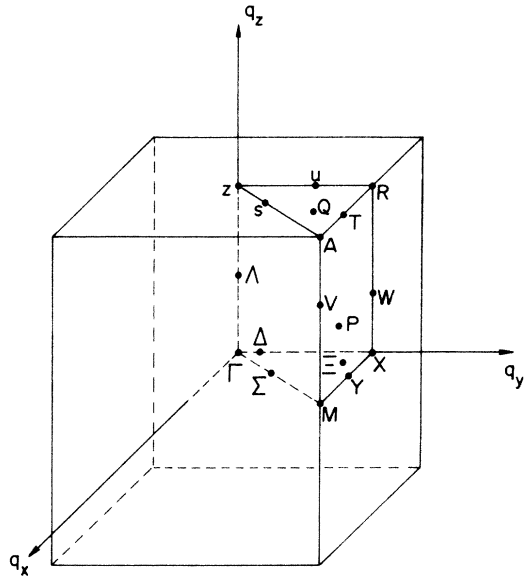

FIG. 1. Brillouin zone for a tetragonal $BaTiO_3$ structure.

III. LATTICE-DYNAMICAL FORMALISM

There are many phenomenological models for the study of lattice dynamics of ionic crystals, such as the rigid-ion model,[38] the shell model,[39,40] the breathing shell model,[41] etc. The use of a model other than a rigid-ion model is rather complex and for crystals with low symmetry and many atoms in the primitive cell they involve a large number of parameters that have to be determined by least-squares analysis of the observed data on frequencies, elastic constants, etc. Such calculations, in general, produce physically unacceptable solutions.[42] The rigid-ion model, on the other hand, does not account for the polarizability of the ions. However, the model is rather simple and in most materials it approximately describes the phonon spectra and the elastic properties of materials. We have, therefore, restricted ourselves to the applicability of the rigid-ion model with the long-range Coulomb and the short-range axially

TABLE I. Classification of normal modes of vibrations at high-symmetry critical points.

Critical point	Symmetry	Normal modes of vibration
Γ,Z,Λ	C_{4v}	$4A_1$(Pb,Ti,O)⊕$5E$(Pb,Ti,O)⊕B_1(O)
R,X,W	C_{2v}	$5A_1$(Pb,Ti,O)⊕$5B_2$(Pb,Ti,O)⊕$3A_2$(Ti,O)⊕$2B_1$(Pb,O)
T,Y	C_s	$7A'$(Pb,Ti,O)⊕$8A''$(Pb,Ti,O)
U,Δ,Ξ	C_s	$10A'$(Pb,Ti,O)⊕$5A''$(Pb,Ti,O)
S,Σ,N	C_s	$9A'$(Pb,Ti,O)⊕$6A''$(Pb,Ti,O)
A,V,M	C_{4v}	$2A_1$(Pb,O)⊕A_2(O)⊕B_1(O)⊕$3B_2$(Ti,O)⊕$4E$(Pb,Ti,O)

TABLE II. Basis vectors for the normal modes of vibrations at high-symmetry critical points.

Critical point	Mode	Basis vectors
Γ	A_1	$\hat{z}_1, \hat{z}_2, \hat{z}_3, \hat{z}_4+\hat{z}_5$
	B_1	$\hat{z}_5-\hat{z}_4$
	E	$\hat{x}_1, \hat{x}_2, \hat{x}_3, \hat{x}_4, \hat{x}_5$
		$\hat{y}_1, \hat{y}_2, \hat{y}_3, \hat{y}_4, \hat{y}_5$
R	A_1	$\hat{z}_1, \hat{y}_2, \hat{y}_3, \hat{y}_5, \hat{z}_4$
	A_2	$\hat{x}_2, \hat{x}_3, \hat{x}_5$
	B_1	$\hat{x}_1, \hat{x}_4$
	B_2	$\hat{y}_1, \hat{y}_4, \hat{z}_2, \hat{z}_3, \hat{z}_5$
T	A'	$\hat{x}_1, \hat{x}_4, \hat{y}_2, \hat{y}_3, \hat{y}_5, \hat{z}_1, \hat{z}_4$
	A''	$\hat{x}_2, \hat{x}_3, \hat{x}_5, \hat{y}_1, \hat{y}_4, \hat{z}_2, \hat{z}_3, \hat{z}_5$
U	A'	$\hat{y}_1, \hat{y}_2, \hat{y}_3, \hat{y}_4, \hat{y}_5, \hat{z}_1, \hat{z}_2, \hat{z}_3, \hat{z}_4, \hat{z}_5$
	A''	$\hat{x}_1, \hat{x}_2, \hat{x}_3, \hat{x}_4, \hat{x}_5$
S	A'	$\hat{x}_1+\hat{y}_1, \hat{x}_2+\hat{y}_2, \hat{x}_3+\hat{y}_3, \hat{x}_4+\hat{y}_5, \hat{x}_5+\hat{y}_4,$ $\hat{z}_1, \hat{z}_2, \hat{z}_3, \hat{z}_4+\hat{z}_5$
	A''	$\hat{x}_1-\hat{y}_1, \hat{x}_2-\hat{y}_2, \hat{x}_3-\hat{y}_3, \hat{x}_4-\hat{y}_5, \hat{x}_5-\hat{y}_4,$ $\hat{z}_4-\hat{z}_5$
A	A_1	$\hat{z}_1, \hat{x}_4+\hat{y}_5$
	A_2	$\hat{x}_5-\hat{y}_4$
	B_1	$\hat{x}_4-\hat{y}_5$
	B_2	$\hat{z}, \hat{z}_3, \hat{x}_5+\hat{y}_4$
	E	$\hat{x}_1, \hat{y}_2, \hat{y}_3, \hat{z}_4$
		$\hat{y}_1, \hat{x}_2, \hat{x}_3, \hat{z}_5$

symmetric interactions.

Following Born and Huang[38] the dynamical matrix is constructed in terms of atomic force constants $\phi_{\alpha\beta}\binom{ll'}{\kappa\kappa'}$ that are second derivatives of the crystal potential energy with respect to the displacement $u_\alpha\binom{l}{\kappa}$ of ion $\binom{l}{\kappa}$ in α direction. The potential energy may be written as the sum of the Coulomb energy ϕ^C and the short-range part ϕ^r. Usually the short-range part is expressed as follows:

$$\phi^r=\alpha e^{-\beta r}\ , \tag{1a}$$

$$\phi^r=\frac{\gamma}{r^n}\ , \tag{1b}$$

where the constants α, β, γ, and n depend on the ion pairs involved and r is the interatomic distance.

A more general approach, called the axially symmetric model, has been introduced in order to represent the short-range interactions, and they involve constants A and B for each ion pair, defined as follows:

$$\left.\frac{1}{r}\frac{\partial\phi^r}{\partial r}\right|_0=\frac{e^2}{2V}B\ , \tag{2a}$$

$$\left.\frac{\partial^2\phi^r}{\partial_r 2}\right|_0=\frac{e^2}{2V}A\ . \tag{2b}$$

The subscript 0 denotes that the derivations are to be calculated at the equilibrium position of the ions. The eigenvalues of the dynamical matrix are the frequencies of the normal modes of vibrations, whereas the eigenvectors of the matrix represent the normal modes themselves. The matrix elements are known as coupling coefficients. In a rigid-ion model[38] the coupling coefficients can be separated into the Coulomb sums and the short-range repulsive part that can be obtained by a Taylor expansion of their respective potential functions. The Coulomb sums were evaluated using the method described by Cowley.[43]

A. Rigid-ion formulation for $PbTiO_3$

The potential energy for the primitive cell of $PbTiO_3$ is written as

$$\begin{aligned}\phi=&-\alpha_M\frac{e^2}{r_0}+4\phi_{13}(r_{13})+4\phi_{14}(r_{14})+4\phi'_{14}(r'_{14})\\&+\phi_{23}(r_{23})+\phi'_{23}(r'_{23})+4\phi_{24}(r_{24})\\&+8\phi_{34}(r_{34})+4\phi_{45}(r_{45})\ ,\end{aligned} \tag{3}$$

where the first term represents the electrostatic energy of the crystal; α_M is the Madelung constant. The remaining terms represent the short-range contributions from various ion pairs. The numbers in front of the short-range–potential constants represent the number of identical interactions, whereas the primed terms represent the next-nearest contributions from the ion pairs with the same identification indices as their unprimed terms.

In the axially symmetric representation of the short-range interaction, the model has 16 short-

range-potential constants, viz., A_{13}, A_{14}, A'_{14}, A_{23}, A'_{23}, A_{24}, A_{34}, A_{45}, B_{13}, B_{14}, B'_{14}, B_{23}, B'_{23}, B_{24}, B_{34}, and B_{45}. The long-range Coulomb interactions require knowledge of the effective charges on the ions. With the use of a charge-neutrality condition we may express the effective charge on a titanium ion as a function of charges on oxygen and lead ions and thus the rigid-ion model involves two charge parameters in addition to the 16 short-range-potential constants mentioned above. This number can, however, be reduced by considering the stability conditions for the unit cell. This requires the precise knowledge of the structural parameters of the crystal. Following Katiyar,[44] the potential energy of the primitive cell is minimized with respect to each structural parameter. In the case of $PbTiO_3$, there are five structural parameters, namely a, c, u, v, and w, and, therefore, five stability conditions may be written, thus reducing the number of unknown short-range-potential constants (B's) from eight to three. The resulting equations are written as

$$4vB_{13}+(v-u)B_{23}+(1+v-u)B'_{23} = 8(w-v)B_{34}+\frac{2V}{c^2}\frac{\partial\alpha_M}{\partial v} , \quad (4a)$$

$$4(w-1)B_{14}+4(w-u)B_{24} = -8(w-v)B_{34}-4wB'_{14}+\frac{2V}{c^2}\frac{\partial\alpha_M}{\partial w} , \quad (4b)$$

$$-(v-u)B_{23}-(1+v-u)B'_{23}-4(w-u)B_{24}=\frac{2V}{c^2}\frac{\partial\alpha_M}{\partial u} , \quad (4c)$$

$$4v^2B_{13}+4(w-1)^2B_{14}+(v-u)^2B_{23}+(1+v-u)^2B'_{23} = -4w^2B'_{14}-8(w-v)^2B_{34}+\frac{2V}{c}\frac{\partial\alpha_M}{\partial c} , \quad (4d)$$

$$2B_{13}+B_{14}+B_{24}=-B'_{14}-2B_{34} -2B_{45}+\frac{2V}{a}\frac{\partial\alpha_M}{\partial a} . \quad (4e)$$

These equations can be utilized to determine five parameters, say B_{13}, B_{14}, B_{23}, B'_{23}, and B_{24}. The number of independent parameters of the model may be reduced further by assuming that the short-range radial force constants for an ion pair are approximated by a Born-Mayer potential, i.e., they are given by

$$A=\beta\alpha^2e^{-\alpha r} . \quad (5)$$

The coefficients can be related to the exponential factors n appearing in Pauling's potential in the following manner:

$$\alpha_1=\alpha_{Pb\text{-}O}=(n_1+1)/r_{14} , \quad (6a)$$

$$\alpha_2=\alpha_{\pi\text{-}O}=(n_2+1)/r_{23} , \quad (6b)$$

$$\alpha_3=\alpha_{O\text{-}O}=(n_3+1)/r_{45} . \quad (6c)$$

The use of the above equations results in the reduction of radial force constants from eight to three as follows:

$$A_{13}=A_{14}\exp[-\alpha_1(r_{13}-r_{14})] , \quad (7a)$$

$$A'_{14}=A_{14}\exp[-\alpha_1(r'_{14}-r_{14})] , \quad (7b)$$

$$A'_{23}=A_{23}\exp[-\alpha_2(r'_{23}-r_{23})] , \quad (7c)$$

$$A_{24}=A_{23}\exp[-\alpha_2(r_{24}-r_{23})] , \quad (7d)$$

$$A_{34}=A_{45}\exp[-\alpha_3(r_{34}-r_{45})] . \quad (7e)$$

Summing up all of the above considerations, the number of unknown parameters for the model are $n_1(n_{Pb\text{-}O})$, n_2(Ti-O), n_3(O-O), A_{14}, A_{23}, A_{45}, B'_{14}, B_{34}, B_{45}, Z_{Pb}, and Z_O. These parameters were determined by nonlinear least-squares analysis of the experimental phonon frequencies at various wave vectors in the Brillouin zone taken from Refs. 21 and 23.

The values of n_1, n_2, and n_3 were taken from Pauling's book.[45] It was noted during the calculations that the variation in the value of n_3 from an initial value of 7 produces insignificant changes in the phonon-frequency fit. We therefore fixed it to 7 as suggested by Pauling[45] for the oxygen-oxygen interactions. The best-fitted values for the remaining ten parameters are as follows: $n_1=5.40$, $n_2=3.15$, $A_{14}=38.01$, $A_{23}=192.80$, $A_{45}=6.33$, $B'_{14}=-2.02$, $B_{34}=-1.38$, $B_{45}=-2.01$, $Z_{Pb}=1.70$, and $Z_O=-1.46$. These values were used to compute axially symmetric short-range force constants and they are listed in Table III. All of the computed parameters appear to be physically acceptable. As expected, the radial constants between the titanium and oxygen ions are large compared to other potential constants, whereas the small values of A_{34} and A_{45} show that the interactions between the oxygen ions are considerably

TABLE III. Force-constant parameters of the rigid-ion model for $PbTiO_3$ at room temperature and at temperatures near the transition point.

Parameter	Room temperature	Transition temperature
A_{13}	19.254	16.868
A_{14}	38.010	37.354
A'_{14}	6.935	7.375
A_{23}	192.800	196.525
A'_{23}	48.893	49.838
A_{24}	122.797	102.369
A_{34}	4.852	3.903
A_{45}	6.266	4.187
B_{13}	−2.623	−3.370
B_{14}	−7.267	−7.507
B'_{14}	−2.024	−1.882
B_{23}	−25.097	−32.024
B'_{23}	−0.491	−1.973
B_{24}	−14.306	−15.725
B_{34}	−1.384	−0.931
B_{45}	−2.007	0.899
Z_{Pb}	1.695e	1.825e
Z_O	−1.456e	−1.433e
Z_{Ti}	2.673e	2.474e

TABLE IV. Observed and computed phonon frequencies for $PbTiO_3$ at room temperature.

Critical point	Mode symmetry	Observed frequency (cm^{-1})	Computed frequency (cm^{-1})
Γ	$A_1(TO_1)$	147	119
	$A_1(TO_2)$	359	301
	$A_1(TO_3)$	646	578
	$E(TO_1)$	88	97
	$E(TO_2)$	220	259
	$E(TO_3)$	289	305
	$E(TO_4)$	505	553
	$A_1(LO_1)$	189	167
	$A_1(LO_2)$	465	514
	$A_1(LO_3)$	796	763
	$E(LO_1)$	128	149
	$E(LO_2)$	289	300
	$E(LO_3)$	439	475
	$E(LO_4)$	723	758
	B_1	289	263
Z	E(TA)	59	50
	E(TO)	168	163
X	A_1(TA)	72	64

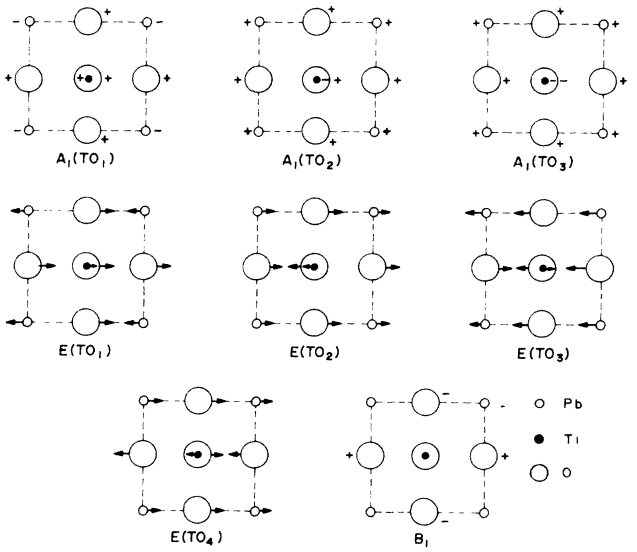

FIG. 2. Graphical representation of zone-center normal modes of vibrations for $PbTiO_3$ with atoms projected on an x-y basal plane. The corner atoms are Pb and the shaded atoms are Ti. The oxygen atoms are shown by large open circles.

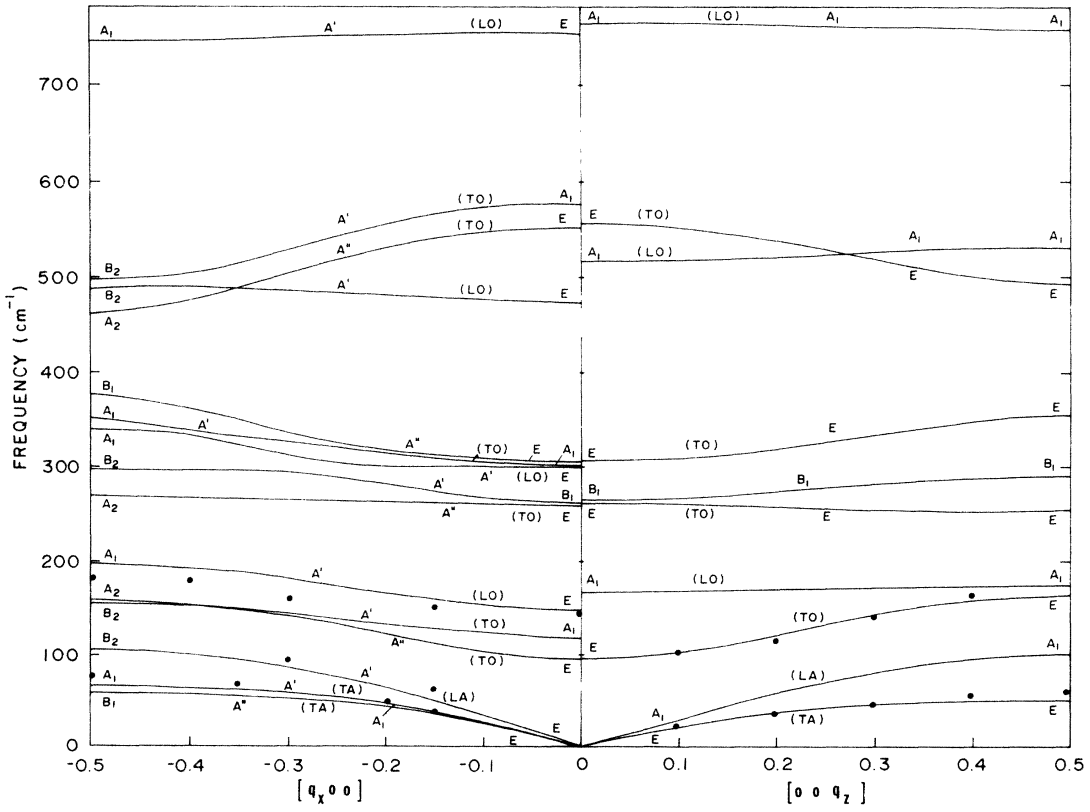

FIG. 3. Computed phonon dispersion curves for $PbTiO_3$ along [100] and [001] directions. The shaded circles denote experimental observations.

weak. The charges on Pb, Ti, and O ions are about 85%, 67%, and 73%, respectively, of their free-ion values. This suggests that the crystal is highly ionic. The values of n_1(Pb-O) and n_2(Ti-O) are considerably smaller than those calculated using the criterion suggested by Pauling for ionic crystals. A comparison between the calculated and experimentally observed phonon frequencies is shown in Table IV. In general, there is good agreement between the observed and the calculated ones, with a maximum disagreement of about 11% in the lowest optic mode. These differences may be explained due to the fact that we have neglected the ionic polarization forces by restricting to the rigid-ion formulation.

The computed eigenvectors were used to find the normal modes of vibrations for the zone-center modes and their graphical representation in two dimensions is shown in Fig. 2. The lowest $E(TO_1)$ and $A_1(TO_1)$ modes need special attention as their frequencies vary considerably with temperature. In the $E(TO_1)$ mode both Ti and O ions move against Pb ions along the x or y axis. Similar movements occur in the soft-mode $A_1(TO_1)$ along the z direction. This description of the soft mode is in agreement with the proposed picture of the normal mode by Last[46] for $BaTiO_3$.

The calculated phonon dispersion curves along [1 0 0] and [0 0 1] are plotted in Fig. 3. The observed points are marked by solid circles. These curves may be useful in carrying out further experimental studies of phonons.[47]

B. Rigid-ion formulation for $BaTiO_3$

The potential energy for the primitive cell of $BaTiO_3$ is written as follows:

$$\phi = -\frac{\alpha_M e^2}{r_0} + 4\phi_{13}(r_{13}) + 4\phi_{14}(r_{14}) + 4\phi'_{14}(r'_{14}) + \phi_{23}(r_{23}) + \phi'_{23}(r'_{23}) + 4\phi_{24}(r_{24}) + 4\phi_{34}(r_{34}) + 4\phi'_{34}(r'_{34}) + 4\phi_{45}(r_{45}) \ . \tag{8}$$

There is a difference between the potential-energy expression used for $PbTiO_3$ and $BaTiO_3$. In $PbTiO_3$, there are eight interactions of type 3–4 with identical separation, whereas in $BaTiO_3$ four of them have slight separation. The approximations used for reducing the unknown number parameters are the same. The potential stability conditions for $BaTiO_2$ may be written as follows:

$$4vB_{13} + (v-u)B'_{23} + (1+v-u)B_{23} = 4(w-v)B'_{34} + 4(w-v-1)B_{34} + \frac{2V}{c^2}\frac{\partial \alpha_M}{\partial v} \ , \tag{9a}$$

$$4(w-1)B'_{14} + 4(w-u)B_{24} = -4(w-v)B'_{34} - 4(w-v-1)B_{34} - 4wB_{14} + \frac{2V}{c^2}\frac{\partial \alpha_M}{\partial w} \ , \tag{9b}$$

$$-(v-u)B'_{23} - (1+v-u)B_{23} - 4(w-u)B_{24} = \frac{2V}{c^2}\frac{\partial \alpha_M}{\partial u} \ , \tag{9c}$$

$$4v^2B_{13} + 4(w-1)^2B'_{14} + (v-u)^2B'_{23} + (1+v-u)^2B_{23} + 4(w-u)^2B_{24} = -4w^2B_{14} - 4(w-v)^2B'_{34} - 4(w-v-1)^2B_{34} + \frac{2V}{c}\frac{\partial \alpha_M}{\partial c} \ , \tag{9d}$$

$$2B_{13} + B'_{14} + B_{24} = -B_{14} - B_{34} - B'_{34} - 2B_{45} + \frac{2V}{a}\frac{\partial \alpha_M}{\partial a} \ . \tag{9e}$$

We utilized the above linear equations to compute B_{13}, B'_{14}, B_{23}, B'_{23}, and B_{24}. The remaining parameters, viz., n_1(Ba-O), n_2(Ti-O), n_3(O-O), A_{14}, A_{23}, A_{34}, B_{14}, B_{34}, B'_{34}, B_{45}, Z_{Ba}, and Z_O were determined by nonlinear least-squares analysis of the observed phonon frequencies using the above model. Just as in the case of $PbTiO_3$, it was necessary to fix the value of n_3 to 7, thus reducing the adjustable parameters to 11. Their best-fitted values are as follows: $n_1 = 5.99$, $n_2 = 3.48$, $A_{14} = 28.28$, $A_{23} = 148.40$, $A_{34} = 5.44$, $B_{14} = -0.82$, $B_{34} = -0.96$, $B'_{34} = -0.46$, $B_{45} = -2.67$, $Z_{Ba} = 1.58$, and $Z_O = -1.42$. The experimental phonon frequencies were taken from the publications by Scalabrin *et al.*,[4] and by Lima *et al.*[7] We did not include the observed zone-boundary phonon frequencies in the fitting procedure in this material. The lowest observed phonon frequency is overdamped, suggesting the presence of large anharmonicity effects.

The computed axially symmetric force constants and the ionic charges for $BaTiO_3$ crystal are shown in Table V. Strong interactions between Ti and O ions are evident from large values of the force constants A_{23}, A'_{23}, and A_{24}. These and the other radial force constants are very similar to those observed in $PbTiO_3$. The large effective ionic charges on Ba(79%), Ti(67%), and O(71%) ions are indicative of predominant ionic character of the crystal. A comparison between the experimental and the calculated zone-center phonon frequencies is made in Table VI. There appears to be a reasonably good agreement between them. The lowest $E(TO_1)$ mode is overdamped in the observed Raman spectrum. Just as in lead titanate, we have deduced the normal modes of

TABLE V. Force-constant parameters of the rigid-ion model for $BaTiO_3$.

r'_{KK}	A'_{KK}	B'_{KK}
r_{13}	26.483	−3.563
r_{14}	28.279	−0.821
r'_{14}	22.854	−0.126
r_{23}	148.399	−42.990
r'_{23}	74.083	−24.917
r_{24}	109.759	−20.599
r_{34}	5.436	−0.958
r'_{34}	4.616	−0.460
r_{45}	5.239	−2.672

$Z_{Ba}=1.582e$ $Z_{Ti}=2.678e$ $Z_O=1.420e$

vibrations for the zone-center optical phonons from the computed eigenvectors, and their graphical representations on the x-y plane are shown in Fig. 4. For $BaTiO_3$ we have plotted only those normal modes of vibrations which differ from $PbTiO_3$.

IV. OBLIQUE DISPERSION OF PHONONS

Studies of the variation of phonon frequencies with the direction of the wave vectors were made by Loudon[48] and Merten.[49] According to Loudon, the variation of phonon frequencies is due to the change in the electrostatic and short-range forces. Two cases were studied in detail. (a) The short-range forces prevail on the electrostatic forces:

$$|\nu(A_{TO})-\nu(E_{TO})| \gg \nu(A_{LO})-\nu(A_{TO}) , \quad (10a)$$

$$|\nu(A_{TO})-\nu(E_{TO})| \gg \nu(E_{LO})-\nu(E_{TO}) . \quad (10b)$$

In this case the following relations are valid:

$$\nu^2=\nu^2(A_{TO})\sin^2\theta+\nu^2(A_{LO})\cos^2\theta , \quad (11a)$$

TABLE VI. Observed and computed zone-center phonon frequencies in $BaTiO_3$.

Mode symmetry	Observed frequency (cm^{-1})	Computed frequency (cm^{-1})
$E(TO_1)$	38	39
$E(TO_2)$	180	196
$E(TO_3)$	308	320
$E(TO_4)$	489	514
$E(LO_1)$	180	182
$E(LO_2)$	308	308
$E(LO_3)$	466	462
$E(LO_4)$	722	699
$A_1(TO_1)$	178	155
$A_1(TO_2)$	267	193
$A_1(TO_3)$	512	554
$A_1(LO_1)$	189	193
$A_1(LO_2)$	473	466
$A_1(LO_3)$	740	729
B_1	308	282

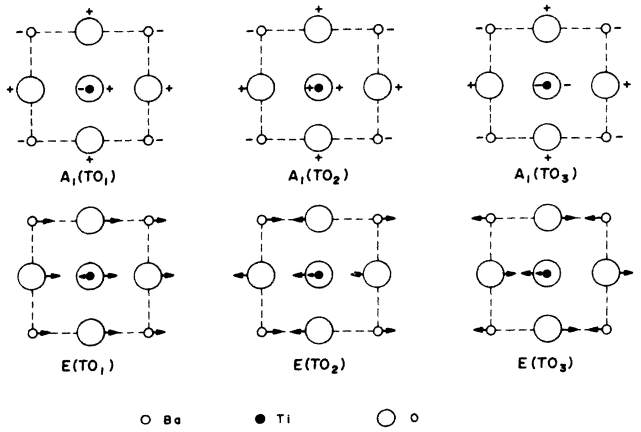

FIG. 4. Graphical representation of zone-center normal modes of vibrations for $BaTiO_3$ with atoms projected on an x-y basal plane. The corner atoms are Ba and the shaded atoms are Ti. The oxygen atoms are shown by large open circles.

$$\nu^2=\nu^2(E_{TO})\cos^2\theta+\nu^2(E_{LO})\sin^2\theta , \quad (11b)$$

where θ is the angle between the c axis and the wave vector of the phonon.

(b) The electrostatic forces prevail on the short-range forces:

$$|\nu(E_{TO})-\nu(A_{TO})| \ll \nu(E_{LO})-\nu(E_{TO}) , \quad (12a)$$

$$|\nu(E_{LO})-\nu(A_{LO})| \ll \nu(A_{LO})-\nu(A_{TO}) . \quad (12b)$$

In this case the following relations are valid:

$$\nu^2=\nu^2(A_{TO})\sin^2\theta+\nu^2(E_{TO})\cos^2\theta , \quad (13a)$$

$$\nu^2=\nu^2(A_{LO})\cos^2\theta+\nu^2(E_{LO})\sin^2\theta . \quad (13b)$$

Equations (11) and (13) are valid for uniaxial crystals with two atoms in the primitive cell. The validity of Loudon's approximation in the case of well-separated phonons from the remaining ones of the same symmetry in $PbTiO_3$ and $BaTiO_3$ was, however, confirmed by computing the phonon frequency variations for very small wave vectors in different directions. Since the electrostatic forces dominate the short-range forces in these crystals, Eq. (13), therefore, should apply in the present cases. The results of the phonon dispersion relations in $PbTiO_3$ for small wave vectors propagating in the k_y-k_z plane are shown in Fig. 5. The experimentally observed points are shown by solid circles.[22] The computed dispersion curves approximate very well Loudon's Eq. (13), except in the region around 300 cm^{-1}, where there are many phonons. The k_y-k_z planes have only mirror symmetry and therefore the phonons at a general point in the plane can be classified as of species A' or A''. It is interesting to note that a crossing of two A' phonons around 300 cm^{-1} occurs. This is because one of the two phonons involved is a nonpolar B_1 mode for small wave vectors strictly along the z or x axis. The oblique dispersion curves for $BaTiO_3$ are shown in Fig. 6. There are no experimental observations available for oblique phonons in $BaTiO_3$ so far.

V. ELASTIC AND PIEZOELECTRIC PROPERTIES

$PbTiO_3$ and $BaTiO_3$ belong to the piezoelectric class of crystals in which applied stress produces an electrical polarization. Depending on the direction of the wave vector and on the piezoelectric tensor, the acoustical wave can be followed by a longitudinal electric field that increases the elastic constants. Hudson and White[50] made a general study of the elastic and electrical properties of the piezoelectric crystals. Following these authors, the differential equations that describe the propagation of an acoustical wave in the [1 0 0] direction is written as

$$\rho\frac{\partial^2 u_i}{\partial t^2}=c'_{1i1k}\frac{\partial^2 u_k}{\partial x_1^2}-e'_{p1i}\frac{\partial E_p}{\partial x_1}\ , \tag{14a}$$

$$\frac{\partial^2 E_p}{\partial x_1^2}=\mu_0\frac{\partial}{\partial t}\left[e'_{p1i}\frac{\partial^2 u_i}{\partial t\,\partial x_1}+\epsilon'_{qp}\frac{\partial E_q}{\partial t}\right]\ , \tag{14b}$$

$$c'_{1i1k}=c_{1i1k}+\frac{l_{11i}l_{11k}}{\epsilon_{11}}\ , \tag{14c}$$

$$e'_{p1i}=-\frac{\epsilon_{p1}}{\epsilon_{11}}e_{11i}+e_{p1i}\ , \tag{14d}$$

$$\epsilon'_{qp}=\epsilon_{qp}-\epsilon_{1p}\frac{\epsilon_{q1}}{\epsilon_{11}}\ , \tag{14e}$$

where c'_{1i1k} is the elastic constant modified by the components of the piezoelectric tensor e_{ijk}, ϵ_{ik} is a component of the dielectric permittivity tensor, ρ is the density of the crystal, and μ_0 is the magnetic permeability. Solutions of the plane-wave type are valid for Eqs. (14a) and (14b),

$$u_i=u_i^0 e^{j(Kx-\omega t)}\ , \tag{15a}$$

$$E_i=E_i^0 e^{j(Kx-\omega t)}\ , \tag{15b}$$

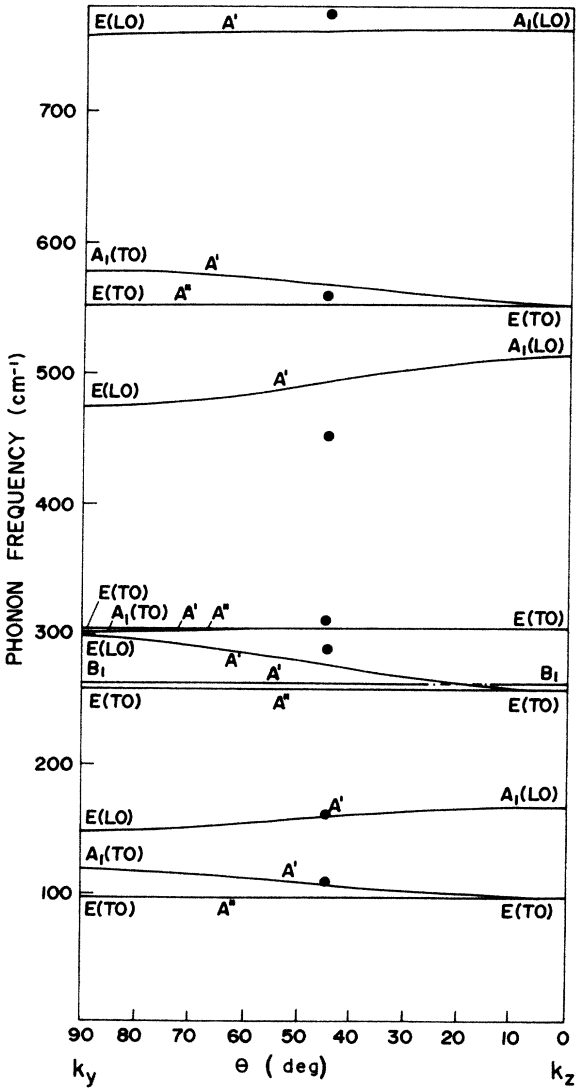

FIG. 5. Oblique phonon dispersion curves for $PbTiO_3$ for small wave vectors in the k_y-k_z plane, with the experimental observations marked by shaded circles.

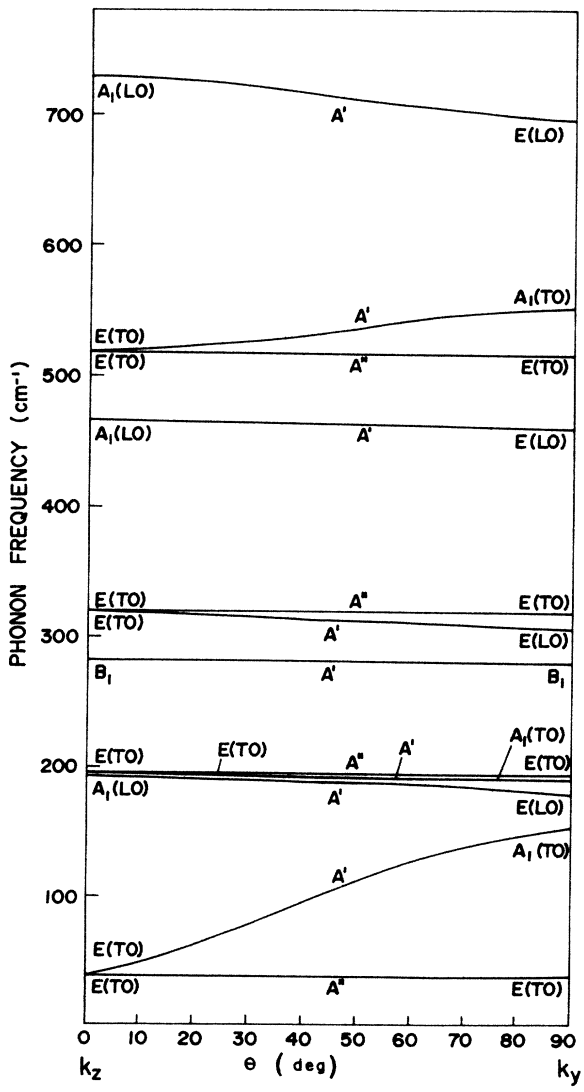

FIG. 6. Oblique phonon dispersion curves for $BaTiO_3$ for small wave vectors in the k_y-k_z plane.

where $K=2\,(q_x/a, q_x/a, q_z/c)$. This choice of solution gives us the following linear equations:

$$\rho\omega^2 u_i^0 = K^2 c'_{1i1k} u_k^0 + jK e'_{q1i} \,, \tag{16a}$$

$$K^2 E_p = j\mu_0 K^2 \omega^2 e'_{p1i} u_i^0 + \mu_0 \omega^2 \epsilon'_{qp} \,. \tag{16b}$$

Hudson and White[50] showed that the correct acoustical-wave solutions can be obtained by solving only Eq. (14a) and neglecting the term $e'_{p1i}(jE_p/jx_1)$ in it:

$$\rho\omega^2 u_i^0 = K^2 c'_{1i1k} u_K^0 \,. \tag{17}$$

The above results can be applied to $PbTiO_3$ and $BaTiO_3$ or any other crystal with C_{4v} symmetry. In what follows a two-index matrix notation will be used for the elastic, piezoelectric, and dielectric tensor components. Equation (17) can be solved for various directions of q. Following are a few cases for which the secular equation was solved to yield the following relations.

(a) $q=(q_x/a, 0, 0)$:

$$c_{11} = \rho v_{\mathrm{LA}}^2(x)/q^2 \,, \tag{18a}$$

$$c_{66} = \rho v_{\mathrm{TA}}^2(y)/q^2 \,, \tag{18b}$$

$$c_{44} + \frac{e_{15}^2}{\epsilon_{11}} = \rho \frac{v_{\mathrm{TA}}^2(z)}{q^2} \,. \tag{18c}$$

(b) $q=(0, 0, q_z/c)$:

$$c_{33} + \frac{l_{33}^2}{\epsilon_{33}} = \rho v_{\mathrm{LA}}^2(z)/q^2 \,, \tag{19a}$$

$$c_{44} = \rho v_{\mathrm{TA}}^2(x)/q^2 \,. \tag{19b}$$

(c) $q=(q_x/a, q_y/a, 0)$:

$$c_{66} + \tfrac{1}{2}(c_{11}+c_{12}) = \rho \frac{v_{\mathrm{LA}}^2(x+y)}{q^2} \,, \tag{20a}$$

$$\tfrac{1}{2}(c_{11}-c_{12}) = \rho v_{\mathrm{TA}}^2(x-y)/q^2 \,, \tag{20b}$$

$$c_{44} + \frac{l_{15}^2}{11} = \rho \frac{v_{\mathrm{TA}}^2(z)}{q^2} \,. \tag{20c}$$

(d) $q=(q_x/a, 0, q_z/c)$: For this wave vector we use the secular determinant, written as

$$\det \begin{vmatrix} M_{11}-\rho\dfrac{v^2}{q^2} & 0 & M_{13} \\ 0 & M_{11}-\rho\dfrac{v^2}{q^2} & 0 \\ M_{13} & 0 & M_{33}-\rho\dfrac{v^2}{q^2} \end{vmatrix} = 0 \,, \tag{21}$$

where

$$M_{11} = \cos^4\theta\, c_{11} + \sin^4\theta\, c_{33} + \cos^2\theta \sin^2\theta(2c_{13}+4c_{44}) + \frac{1}{\epsilon}[\sin^2\theta\, e_{33} + \cos^2\theta \sin\theta(2e_{15}+e_{31})]^2 \,, \tag{22a}$$

$$M_{13} = \cos^3\theta \sin\theta(c_{11}-c_{13}-2c_{44}) + \cos\theta \sin^2\theta(c_{13}-c_{33}+2c_{44}) - \frac{1}{\epsilon}\{[\cos^3\theta\, e_{15} + \cos\theta \sin^2\theta(e_{33}-e_{15}-e_{31})][\cos^2\theta \sin\theta(2e_{15}+e_{31}) + \sin^3\theta\, e_{33}]\} \,, \tag{22b}$$

$$M_{22} = \cos^2\theta\, c_{66} + \sin^2\theta\, c_{44} \,, \tag{22c}$$

$$M_{33} = \cos^2\theta \sin^2\theta(c_{11}-2c_{13}-2c_{44}+c_{33}) + \cos^4\theta\, c_{44} + \sin^4\theta\, c_{44} + \frac{1}{\epsilon}[\cos^3\theta\, e_{15} + \cos\theta \sin^2\theta(e_{33}-e_{15}-e_{31})]^2 \,, \tag{22d}$$

$$\epsilon = \cos^2\theta\, \epsilon_{11} + \sin^2\theta\, \epsilon_{33} \,, \tag{22e}$$

with

$$\cos\theta = \frac{q_x/a}{[(q_x/a)^2+(q_z/c)^2]^{1/2}}$$

and

$$\sin\theta = \frac{q_z/c}{[(q_*/a)^2+(q_z/c)^2]^{1/2}} \,.$$

Equation (21) gives the following results:

$$\rho \frac{v_{\mathrm{TA}}^2(y)}{q^2} = \cos^2\theta\, c_{66} + \sin^2\theta\, c_{44} \,, \tag{23a}$$

$$v_{\pm}^2 = \tfrac{1}{2}(M_{11}+M_{33})\frac{q^2}{\rho^2} \pm \frac{q^2}{\rho^2}[(M_{11}+M_{33})^2]^{1/2} - 4(M_{11}M_{33}-M_{13}^2) \,, \tag{23b}$$

where $v_+ = v_{\mathrm{LA}}(xz)$, $v_- = v_{\mathrm{TA}}(xz)$.

The above results can be conveniently applied to study elastic, dielectric, and piezoelectric properties of $PbTiO_3$ and $BaTiO_3$. Let us first consider the case of a $PbTiO_3$ crystal. The measurements of elastic and piezoelectric constants for $PbTiO_3$ were made in polycrystalline samples.[29] The only measurement of the static dielectric constant ϵ_{33} was made by Bhide *et al.*,[32] giving the value $\epsilon_{33}=30$. Frey and Silberman,[22] using the Layddane-Sachs-Teller (LST) relation, obtained the values $\epsilon_{11}=125.6$ and $\epsilon_{33}=30.4$. The calculations of the elastic and piezoelectric constants were made by computing the frequencies of the normal modes of the dynamical matrix. The value of q_x used was 0.05. For waves propagating in direction [0 0 1], q_z was fixed at 0.05. For waves propagating in direction [1 0 1], a choice of the values of q_z was made giving the angles

TABLE VII. Observed and computed elastic, dielectric, and piezoelectric constants for $PbTiO_3$.

c_{ij}	Observed values c_{ij} (10^{11} N/m^2)	Computed values c_{ij} (10^{11} N/m^2)
c_{11}	1.433	1.327
c_{12}	0.322	0.846
c_{13}	0.241	0.891
c_{33}	1.316	0.934
c_{44}	0.558	0.801
c_{66}	0.556	0.927
d_{ij}	d_{ij} (10^{-12}/N)	d_{ij} (10^{-12}/N)
d_{15}	53.0	45.521
d_{31}	−4.4	−15.070
d_{33}	51.0	51.000
ϵ_{ij}/ϵ_0	ϵ_{ij}/ϵ_o	ϵ_{ij}/ϵ_0
ϵ_{11}/ϵ_0	230 (125.6)	125.6
ϵ_{33}/ϵ_0	170 (30.0)	30.0

30°, 45°, and 60°.

Some of the equations mentioned above relate the same elastic constants to different acoustical-wave frequencies. The calculations show that the results of these equations are compatible, showing that the potential energy of the crystal for the ions in the equilibrium position is a minimum. The elastic piezoelectric and dielectric constants were obtained by utilizing the above equations for various values of θ (30°, 45°, and 60°). These quantities were obtained by adjusting the frequencies of the acoustical waves calculated from the dynamical matrix for the wave vectors considered. The preliminary results showed a high correlation between the parameters e_{33}, e_{31}, ϵ_{11}, and ϵ_{33}. This was due to the fact that the product of these constants give a small correction to the elastic constants. Therefore the parameters e_{11}, e_{33}, and ϵ_{11} were fixed during the least-squares analysis. The experimental value of ϵ_{11} was taken from the work by Frey and Silberman.[22] A comparison of the experimental and calculated values of the elastic, dielectric, and piezoelectric constants is shown in Table VII. The values in parentheses are the values for single crystals. The differences between the experimental and calculated values may be due to the fact that the measurements were made in polycrystalline samples. The same formalism was applied to compute the above constants for a $BaTiO_3$ crystal and the results are compared with the experimental values in Table VIII.[51] The experimental values were obtained in multidomain samples of $BaTiO_3$ (Ref. 52) instead of a single crystal. This may explain the differences between the experimental and calculated values of the elastic constants. The values in parentheses in Table VIII were obtained by Devonshire.[53] The elastic constants calculated by Devonshire agree with the present calculations, with the exception of c_{44}.

TABLE VIII. Observed and computed elastic, dielectric, and piezoelectric constants for $BaTiO_3$.

c_{ij}	Observed values c_{ij} (10^{11} N/m^2)	Computed values c_{ij} (10^{11} N/m^2)
c_{11}	2.751 (1.618)	1.544
c_{12}	1.789 (0.818)	1.154
c_{13}	1.515 (0.861)	0.973
c_{33}	1.648 (1.039)	1.399
c_{44}	0.543 (0.185)	0.743
c_{66}	1.131 (1.234)	1.152
d_{ij}	d_{ij} (10^{-12}/N)	d_{ij} (10^{-12}/N)
d_{15}	392.0 (1160)	286.110
d_{31}	−34.5 (−63)	−36.915
d_{33}	85.6 (165)	85.600
ϵ_{ij}/ϵ_0	ϵ_{ij}/ϵ_o	ϵ_{ij}/ϵ_0
ϵ_{11}/ϵ_0	1970 (600)	1970
ϵ_{33}/ϵ_0	109 (90)	109

VI. VARIATION OF PHONON FREQUENCIES OF $PbTiO_3$ WITH TEMPERATURE

The calculations presented in this work are based on the harmonic approximation, in which the potential energy is expanded to second-order terms. In this approximation the crystals do not have temperature-dependent properties. Following Cochran[10] and Cowley[42] we make some of the crystal parameters a_0 and c_0, the short-

TABLE IX. Observed and computed zone-center phonon frequencies in $PbTiO_3$ near the transition temperature.

Mode symmetry	Observed frequency (cm^{-1})	Computed frequency (cm^{-1})
E(TO)	54	52
E(TO)	178	207
E(TO)	490	535
E(TO)	289	269
E(LO)	118	135
E(LO)	445	467
E(LO)	665	719
E(LO)	289	261
A_1(TO)	62	77
A_1(TO)	289	277
A_1(TO)	545	529
A_1(LO)	163	156
A_1(LO)	445	494
A_1(LO)	725	715
B_1	289	285

range force constants, and the ionic charges are temperature dependent. Near the transition temperature the lattice parameters are[54] $a=3.942$ Å and $c=4.011$ Å in $PbTiO_3$. Measurements of temperature-dependent phonon frequencies for the $PbTiO_3$ crystal were made by Burns and Scott.[19]

We have carried out a least-squares analysis of the phonon frequencies for temperatures near T_c. In the model considered the parameters n_1, n_2, and n_3 were assumed to be temperature independent. A comparison between the experimental and calculated phonon frequencies for $T=T_c$ is shown in Table IX. We note that, in general, the frequencies of the dipolar modes changed with the temperature. The frequency of the $E_1(TO_1)$ mode changed from 97 to 52 cm^{-1}, and the frequency of the $A_1(TO_1)$ mode changed from 119 to 77 cm^{-1}. In the cubic phase, above the transition temperature the frequencies of these modes are identical to the form of the triply degenerate F_{1u} mode. The eigenvectors of the $A_1(TO_1)$ mode show that this mode can be considered responsible for the tetragonal-cubic phase transition in $PbTiO_3$. From a close observation of the parameters of the model listed in Table III, we notice that the variation of the parameters with temperature is small. We may, therefore, conclude that the influence of anharmonic forces on the normal modes of vibrations of this crystal is small. This is similar to what is observed by Cowley[42] in $SrTiO_3$.

VII. CONCLUSIONS

The rigid model was applied to the ferroelectric crystals of $PbTiO_3$ and $BaTiO_3$, in the tetragonal phase. Reasonably good agreement between the calculated and experimentally observed phonon frequencies were obtained. The greater differences between the experimental and calculated frequencies occurred in the polar modes. Improvements in the calculations can be obtained by considering the ionic polarizabilities in the model. We have, however, not attempted to do so because of, in particular, a large number of parameters involved in such considerations. Such calculations often result in some parameters that may not have any physical significance. As an example we can mention the $SrTiO_3$ crystal.[42,55] The shell charges obtained for this crystal have no physical meaning. Similar situations may arise in crystals of $PbTiO_3$ and $BaTiO_3$ using the shell model. Phonon dispersion curves were obtained and the results are in good agreement with the available experimental data. The oblique phonon dispersion curves were obtained for both crystals.

In the computation of elastic and piezoelectric constants it was observed that some discrepancies exist between experimental and calculated values. These observations may be due to the fact that the experimental constants were obtained in polycrystalline samples. The literature search for several other materials shows that there is, in general, a large difference in elastic and piezoelectric constants of single-crystal samples and those of polycrystalline samples. A least-squares fit of the phonon frequencies for temperatures near the phase transition shows that the anharmonic forces present in the $PbTiO_3$ crystal are small.

Finally, we comment on the normal modes shown in Figs. 2 and 4. The graphical representation of the low-frequency $E(TO_1)$ mode shown in Fig. 2 for $PbTiO_3$ is identical to that proposed by Last[46] for $BaTiO_3$. It, however, differs from the $E(TO_1)$ mode of $BaTiO_3$ shown in Fig. 4, which is identical to that proposed by Slater[47] for the soft mode in $BaTiO_3$.

ACKNOWLEDGEMENTS

The research grants from Fundação de Amparo e Pesquisa do Estado de São Paulo and National Science Foundation are gratefully acknowledged.

*On leave from Universidade Estadual de Campinas, Caixa Postal 1170, 13 100 Campinas, São Paulo, Brazil.

[1]F. Jona and G. Shirane, *Ferroelectric Crystals* (MacMillan, New York, 1962).
[2]R. Migoni, H. Bilz, and D. Bauerle, Phys. Rev. Lett. **37**, 1155 (1976).
[3]G. Burns and F. H. Dacol, Phys. Rev. B **18**, 5750 (1978).
[4]A. Scalabrin, A. S. Chaves, D. S. Shim, and S. P. S. Porto, Phys. Status Solidi B **79**, 731 (1977).
[5]A. S. Chaves, R. S. Katiyar, and S. P. S. Porto, Phys. Rev. B **10**, 3522 (1974).
[6]A. Scalabrin, S. P. S. Porto, H. Vargas, C. A. S. Lima, and L. C. M. Miranda, Solid State Commun. **24**, 291 (1977).
[7]C. A. S. Lima, A. Scalabrin, L. C. M. Miranda, H. Vargas, and S. P. S. Porto, Phys. Status Solidi **86**, 373 (1978).
[8]J. A. Sanjurjo, R. S. Katiyar, and S. P. S. Porto, Phys. Rev. B **22**, 2396 (1980).
[9]A. Pinczuk, E. Burstein, and S. Ushioda, Solid State Commun. **7**, 139 (1969).
[10]W. Cochran, Adv. Phys. **9**, 387 (1960).
[11]P. W. Anderson, Izv. Akad. Nauk SSSR, Ser. Fiz. 1603 (1960).
[12]G. Shirane, S. Hoshino, and K. Suzuki, Phys. Rev. **80**, 1105 (1950).
[13]R. J. Nelmes and W. F. Kuhs, Solid State Commun. **54**, 721 (1985).
[14]J. P. Remeika and A. M. Glass, Mater. Res. Bull. **5**, 37 (1970).
[15]J. Kobayashi and R. Ueda, Phys. Rev. Lett. **99**, 1900 (1955).
[16]J. Kobayashi, S. Okamoto, and R. Ueda, Phys. Rev. Lett. **103**, 830 (1956).
[17]J. Kobayashi, Y. Uesu, and Y. Sakemi, Phys. Rev. B **28**, 3866 (1983).
[18]N. E. Tornberg and C. H. Perry, J. Chem. Phys. **53**, 2946 (1970).
[19]G. Burns and B. A. Scott, Phys. Rev. Lett. **25**, 167 (1970).
[20]R. A. Frey, in *Advances in Raman Spectroscopy*, edited by J. P. Mathieu (Heyden, London, 1973), Vol. I.
[21]G. Burns and B. A. Scott, Phys. Rev. B **7**, 3088 (1973).
[22]R. A. Frey and E. Silberman, Helv. Phys. Acta **49**, 1 (1976).

[23]C. H. Perry, B. N. Khana, and G. Rupprecht, Phys. Rev. **135**, A408 (1964).
[24]G. Shirane, J. D. Axe, J. Harada, and J. P. Remeika, Phys. Rev. B **2**, 155 (1970).
[25]D. Heiman and S. Ushioda, Phys. Rev. B **9**, 3616 (1978).
[26]G. Burns, Phys. Rev. Lett. **37**, 229 (1976).
[27]J. A. Sanjurjo, E. Lopez-Cruz, and G. Burns, Phys. Rev. B **28**, 7260 (1983).
[28]T. Nakamura, M. Takashige, H. Tereauchi, Y. Muira, and W. N. Lawless, Jpn. J. Appl. Phys. **23**, 1265 (1984).
[29]S. Ikegami, I. Ueda, and T. Nagata, J. Acoust. Soc. Am. **50**, 1060 (1971).
[30]N. Ichinose and T. Takahashi, Jpn. J. Appl. Phys. **11**, 1224 (1972).
[31]I. Ueda and S. Ikegami, Jpn. J. Appl. Phys. **7**, 236 (1968).
[32]V. G. Bhide, K. G. Deskmukh, and M. S. Hedge, Physica **28**, 871 (1962).
[33]G. Shirane, R. Pepinsky, and B. C. Fraser, Acta Crystallogr. **9**, 131 (1956).
[34]H. D. Megaw, Proc. Phys. Soc. London **58**, 10 (1946).
[35]J. Harada, T. Pedersen, and Z. Barnea, Acata Crystallogr. Sect. A **26**, 336 (1970).
[36]R. G. Rhodes, Acta Crystallogr. **4**, 105 (1951).
[37]H. Montgomery, Proc. R. Soc. London, Ser. A **309**, 521 (1969).
[38]M. Born and K. Huang, *Dynamical Theory of Crystal Lattices, International Series of Monographs on Physics* (Oxford University Press, New York, 1966).
[39]A. D. Woods, W. Cochran, and B. N. Brockhouse, Phys. Rev. New York, **119**, 980 (1960).
[40]R. A. Cowley, W. Cochran, B. N. Brockhouse, and A. D. Woods, Phys. Rev. **131**, 1030 (1963).
[41]U. Schroder, Solid State Commun. **4**, 347 (1966).
[42]R. A. Cowley, Phys. Rev. **134**, A981 (1964).
[43]R. A. Cowley, Acta Crystallogr. **15**, 687 (1962).
[44]R. S. Katiyar, J. Phys. C **3**, 1087 (1970).
[45]L. Pauling, *The Nature of the Chemical Bond* (Cornell University Press, Ithaca, 1960).
[46]J. T. Last, Phys. Rev. **105**, 1740 (1957).
[47]J. C. Slater, Phys. Rev. **78**, 748 (1950).
[48]R. Loudon, Adv. Phys. **13**, 423 (1964).
[49]L. Merten, Z. Naturforsch, **15a**, 47 (1962).
[50]A. R. Hudson and D. L. White, J. Appl. Phys. **33**, 40 (1962).
[51]J. F. Nye, *Physical Properties of Crystals* (Oxford University Press, New York, 1964).
[52]D. Berlincourt and H. Jaffe, Phys. Rev. **111**, 143 (1958).
[53]A. F. Devonshire, Philos. Mag. Suppl. **3**, 85 (1954).
[54]G. Shirane and S. J. Hoshino, J. Phys. Soc. Jpn. **6**, 265 (1951).
[55]W. G. Stirling, J. Phys. C **5**, 2711 (1972).